

Reaction Mechanism of Heavy-Ion Charge-Exchange Scattering at Intermediate Energies

H. Lenske and H. H. Wolter

Sektion Physik, Universität München, K-8046 Garching, West Germany

H. G. Bohlen

Hahn-Meitner-Institut, Berlin, West Germany

(Received 6 December 1988)

The reaction mechanism of heavy-ion charge-exchange scattering at low and intermediate incident energies is studied theoretically. Contributions of direct charge exchange due to central and tensor isovector interactions and of charge exchange via sequential proton and neutron transfer are taken into account in one-step and two-step exact-finite-range distorted-wave Born-approximation calculations. The nuclear structure of the intermediate and final states is described within the shell model. Calculations for $^{12}\text{C}(^{12}\text{C}, ^{12}\text{N})^{12}\text{B}$ indicate that direct charge exchange is safely dominant for incident energies $E/A \gtrsim 100$ MeV.

PACS numbers: 25.70.Cd, 24.50.+g

Charge-exchange scattering has become a very useful new application of heavy-ion physics aiming at spectroscopic studies of both proton-neutron (p,n) and neutron-proton (n,p) type transitions in nuclei. However, the interpretation of such data is complicated because the final channels can be populated by the two distinct reaction mechanisms of direct and transfer charge exchange. In the direct process the final states are excited by the one-step exchange of charged mesons as described by the isovector nucleon-nucleon (NN) interaction. The transfer charge-exchange mechanism is at least a second-order process in which the same final states are populated by sequential proton-pickup neutron-stripping processes (or vice versa). Since the desired nuclear structure information is most directly available from the direct process it is of particular importance to know in which energy range the direct mechanism will dominate.

Single-charge-exchange reactions have been widely studied at incident energies around $E/A = 10$ MeV with light (e.g. Refs. 1-3) and medium-heavy systems⁴⁻⁶ and also in the Fermi-energy regime⁷⁻⁹. It has been found⁵⁻⁸ that at low incident energies $E/A \sim 10$ MeV the transfer contributions generally dominate. Recently, Winfield *et al.*⁷ concluded from the analysis of the reaction $^{12}\text{C}(^{12}\text{C}, ^{12}\text{N})^{12}\text{B}$ at incident energies $10 \text{ MeV} \leq E/A \leq 35 \text{ MeV}$ that only for energies well above 50 MeV will direct charge exchange begin to dominate. However, this result was obtained with rather drastic approximations to the reaction dynamics.

In this Letter we present a quantitative analysis of the energy dependence of the reaction mechanism of heavy-ion charge-exchange scattering. The one-step direct and the two-step transfer contributions are calculated in the first- and second-order distorted-wave Born approximation (DWBA). Nuclear structure is described microscopically by shell-model calculations. A realistic NN interaction including the tensor interaction is used. A

similar approach was successfully applied before to heavy-ion charge-exchange reactions at low incident energies.^{5,6} Here, the reaction mechanism of charge-exchange collisions at incident energies of $10 \text{ MeV} \leq E/A \leq 100 \text{ MeV}$ is studied for the reaction $^{12}\text{C}(^{12}\text{C}, ^{12}\text{N})^{12}\text{B}$. The calculations are compared to data measured recently at the VICKSI accelerator in Berlin with the Q3D spectrometer for $E/A = 30$ MeV and the GANIL accelerator in France with the SPEG spectrometer for $E/A = 70$ MeV. A preliminary report on the measurements has been given in Ref. 10.

The cross section for a charge-exchange reaction

$$a(N_a, Z_a) + A(Z_A, N_A) \rightarrow b(N_a \pm 1, Z_a \mp 1) + B(N_A \mp 1, Z_a \pm 1)$$

is determined by the coherent superposition of direct and transfer charge-exchange contributions. The direct component is described in lowest order by the DWBA T -matrix element¹¹ $T_{\beta\alpha}^{(1)} = \langle \chi_{\beta}^{(-)} | F_{\beta\alpha} | \chi_{\alpha}^{(+)} \rangle$ where $\chi_{\alpha}^{(+)}$ and $\chi_{\beta}^{(-)}$ are the distorted waves in the incident channel $\alpha = (a, A)$ and the final charge-exchange channel $\beta = (b, B)$, respectively. The form factors

$$F_{\beta\alpha}(\mathbf{R}) = \int d\xi_a d\xi_A \rho_{ab}(\xi_z) \rho_{AB}(\xi_A) V^{(\tau)}(\mathbf{R}, \xi_a, \xi_A) \quad (1)$$

are given by folding the isovector NN interaction $V^{(\tau)}$ with the transition densities ρ . Central spin-scalar ($\Delta S = 0$) and spin-vector ($\Delta S = 1$) and also tensor interactions are included in $V^{(\tau)}$. The energy dependence of $V^{(\tau)}$ was taken into account by interpolation between the G -matrix interaction of Anantaraman, Toki, and Bertsch¹² at $E_{NN} \leq 10$ MeV and the complex NN T -matrix interaction of Franey and Love¹³ given at (discrete) NN energies $E_{NN} = 50$ MeV. Single-nucleon knock-out exchange contributions are included in the local-momentum approximation.^{10,14}

The transition densities in Eq. (1) were constructed

with the one-body transition amplitudes of Winfield *et al.*⁷ obtained in $(1p)$ and $(1p, 2s, 1d)$ shell-model calculations for the 1^+ and 2^-4^- states, respectively. The β -decay matrix elements for $^{12}\text{B}(1^+, \text{g.s.})$ and $^{12}\text{N}(1^+, \text{g.s.})$ are very accurately reproduced. Single-particle wave functions were calculated in Wood-Saxon potentials.

The transfer charge-exchange contributions are described, in second-order DWBA, as the superposition of proton-pickup-neutron-stripping and neutron-stripping-proton-pickup processes. The two-step transfer matrix elements are given by^{5,8}

$$T_{\beta\alpha}^{(2)} = \sum_{\gamma} C_{\beta\gamma\alpha} \langle \chi_{\beta}^{(-)} | F_{\beta\gamma} G_{\gamma}^{(+)} F_{\gamma\alpha} | \chi_{\alpha}^{(+)} \rangle. \quad (2)$$

The summation is restricted to intermediate transfer channels γ in which either the particle or the hole com-

ponent of the final configurations are populated. In the present calculations all contributions from $^{13}\text{N} + ^{11}\text{B}$ and $^{11}\text{C} + ^{13}\text{C}$ channels with $(1p, 2s, 1d)$ configurations obeying the above rule have been included so that within the model space the two-step contributions are completely accounted for. Contributions from outside the model space will be strongly suppressed in the final configuration and hence in the cross section because of an energy separation of $2\hbar\omega \gtrsim 25$ MeV. The transfer matrix elements are calculated in second-order exact-finite-range (EFR) DWBA using the prior-post representation.¹⁵ The EFR form factors are denoted by F and the propagation in the intermediate channels is described by the optical model Green's functions $G_{\gamma}^{(+)}$.^{10,15} The amplitudes $C_{\beta\gamma\alpha}$ contain the spectroscopic factors of the first and second steps,^{5,8} respectively, which were taken from shell-model calculations.^{4,7} In contrast to former calculations^{5,8} and to other approaches^{4,7}, here the coherence of the direct and transfer contributions is taken into account, $\sigma_{\beta\alpha} \sim |T_{\beta\alpha}^{(1)} + T_{\beta\alpha}^{(2)}|^2$. Optical potentials from the literature have been used.¹⁶

Theoretical results for the reaction $^{12}\text{C}(^{12}\text{C}, ^{12}\text{N}(1^+, \text{g.s.}))^{12}\text{B}$ at incident energies $10 \text{ MeV} \leq E/A \leq 100$ MeV are shown in Figs. 1 and 2 for angular distributions and excitation functions. In Fig. 1 it is seen that the reaction leading to $^{12}\text{B}(1^+, \text{g.s.})$ is dominated by the transfer contribution for low incident energies. At $E/A=45$ MeV the two contributions are of similar strength at forward angles. The range of angles where the direct process dominates increases with incident energy. However, because of the two-step origin, the transfer angular distributions have a less steep slope and are dominating at larger angles even at $E/A=70$ MeV. Similar results are found for the angular distributions of other final states (see also Fig. 2).

For $E/A=30$ and 70 MeV the calculations are compared to experimental data¹⁰ which are well described without renormalization, thus confirming the reliability of the approach. In this case only intermediate routes with $(1p)$ configurations contribute. The data of Winfield *et al.*⁷ at $E/A=35$ MeV are reproduced equally well.

The incident energy dependence of the peak differential cross section σ_{max} and the angle-integrated cross section σ_{tot} for $^{12}\text{B}(1^+, \text{g.s.})$ and the strongly excited $(2^-, 4^-)$ doublet at $E_x \sim 4.5$ MeV are shown in Fig. 2. Of particular interest is the energy dependence of the direct and transfer contributions, also shown in Fig. 2 separately. The transfer cross sections have their maximum at about $E/A=30$ MeV and then decrease. The direct cross sections, generally, increase with incident energy but depend in detail on the final state. For σ_{max} the crossing point of transfer and direct cross sections is found at $E/A \sim 50$ MeV for the 1^+ and the 2^- states but is shifted to ~ 75 MeV for the 4^- state. In σ_{tot} the crossing points are shifted to higher energies such that they are located at $E/A \sim 60$ MeV for $^{12}\text{B}(1^+)$ and at

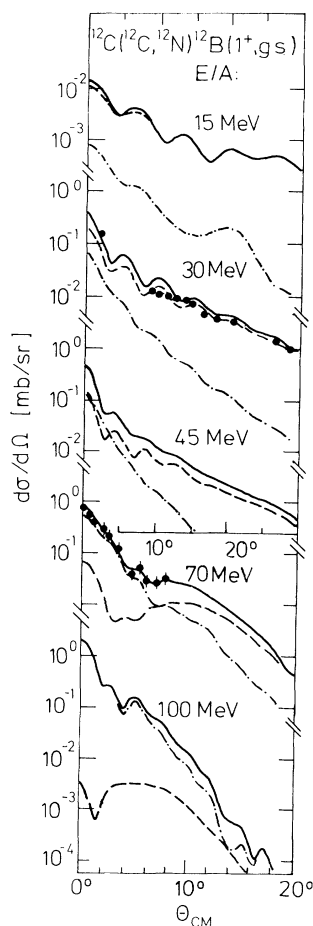


FIG. 1. Angular distributions for $^{12}\text{C}(^{12}\text{C}, ^{12}\text{N}(1^+, \text{g.s.}))^{12}\text{B}(1^+, \text{g.s.})$ at incident energies $10 \text{ MeV} \leq E/A \leq 100$ MeV. Theoretical results for the direct (dashed-dotted lines) and transfer (dashed lines) charge-exchange contributions and also of the coherent sum of both (full lines) are shown. The theory is compared to data (circles) at $E/A=30$ and 70 MeV (Ref. 10). Note the change in abscissa for $E/A=70$ and 100 MeV.

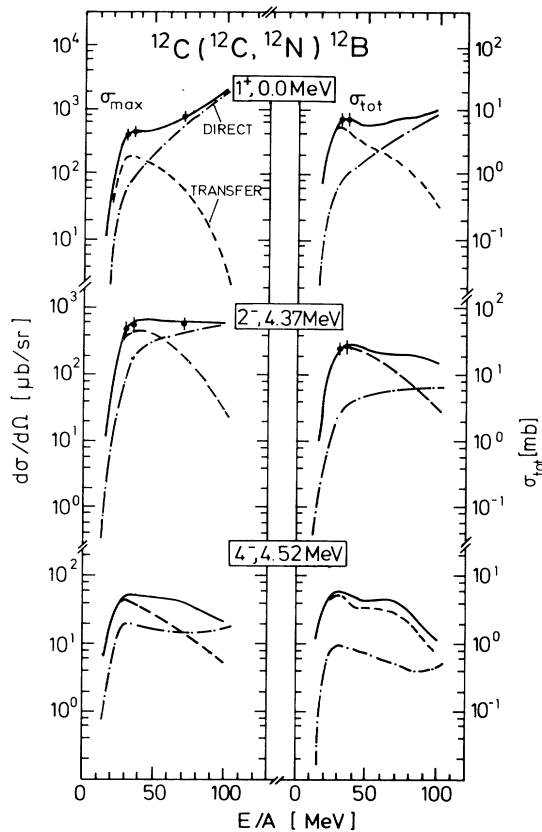


FIG. 2. The maximum of the differential cross section (left) and the total cross sections (right) for $^{12}\text{C}(^{12}\text{C}, ^{12}\text{N})^{12}\text{B}$ as a function of the incident energy per nucleon, E/A . Results are shown for $^{12}\text{B}(1^+, \text{g.s.})$, $^{12}\text{B}(2^-, 4.37 \text{ MeV})$, and $^{12}\text{B}(4^-, 4.52 \text{ MeV})$. The direct (full lines) and transfer (dashed lines) partial cross sections and the coherent sum (bold lines) are displayed. Experimental and theoretical results for the 1^+ and 2^- state are compared at $E/A=30 \text{ MeV}$ (Ref. 10), 35 MeV (Ref. 7), and 70 MeV (Ref. 10).

$E/A=80 \text{ MeV}$ for $^{12}\text{B}(2^-)$ and even at $E/A > 100 \text{ MeV}$ for $^{12}\text{B}(4^-)$. This state dependence is mainly due to the different angular and linear momentum transfers involved in the three cases shown in Fig. 2. The different behavior of σ_{max} and σ_{tot} on incident energy follows from the contribution of the two-step transfer angular distributions at large angles as discussed above.

In Ref. 7 the crossing point in σ_{tot} for $^{12}\text{B}(1^+)$ was estimated to be around $E/A=50 \text{ MeV}$. Although this value agrees rather well with our result there are considerable differences in the detailed energy dependence of the direct and the transfer cross sections in Fig. 2 and the approximate calculations of Winfield *et al.*⁷

The energy dependence of direct and transfer charge exchange can be understood from quite general properties of the two amplitudes. The direct amplitude depends mainly on the momentum transfer (i.e., excitation energy and scattering angle) of the reaction while, as

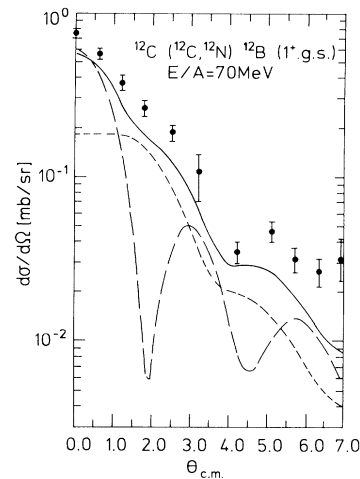


FIG. 3. Direct charge-exchange differential cross section for $^{12}\text{C}(^{12}\text{C}, ^{12}\text{N})^{12}\text{B}(1^+, \text{g.s.})$ at $E/A=70 \text{ MeV}$. The central (long-dashed line) and tensor (short-dashed line) contributions and the coherent sum of both (full line) are shown. The experimental data are taken from Ref. 10.

was discussed by von Oertzen¹⁷ in a plane-wave picture, the transfer amplitudes for each step depend mainly on the linear momenta (i.e., kinetic energy) of the transferred nucleons. These momenta have to be absorbed by the binding potentials. Since high-momentum components are strongly suppressed in the nuclear mean field the transfer cross section will decrease with incident energy as seen in Fig. 2. Since the momentum transfer at a given angle decreases with incident energy the $\Delta L=0$ direct component in the $^{12}\text{B}(1^+)$ reaction is kinematically favored and the cross section continues to increase. This kinematical enhancement is missing for the higher multiplicities so that the cross sections for $^{12}\text{B}(2^-)$ level off and for $^{12}\text{B}(4^-)$ even start to decrease at $E/A \approx 50 \text{ MeV}$.

In order to relate heavy-ion charge-exchange data to β -decay strengths¹⁸ it is important to investigate the direct transition operator in more detail. In Fig. 3 the central and tensor contributions to the direct cross section for $^{12}\text{B}(1^+, \text{g.s.})$ at $E/A=70 \text{ MeV}$ are shown. It is seen that the central interaction results in a strongly oscillatory angular distribution in clear disagreement with the data. The shape of the experimental angular distribution is only reproduced if central and tensor contributions are included coherently (they interfere slightly destructively).

The angular range shown in Fig. 3 corresponds to linear momentum transfers of $0.4 \text{ fm}^{-1} \lesssim q \lesssim 1.4 \text{ fm}^{-1}$. The tensor contributions account for about 33% of the differential cross section at 0° (Fig. 3) and for even 50% of the angle-integrated cross section. They become even more important for higher multiplicities and, for example, contribute by about 70% to the $^{12}\text{B}(2^-)$ cross section. These results reflect the rapid increase of the ten-

tor strength at small momenta $0 < q \lesssim 1 \text{ fm}^{-1}$. A direct relation to the nuclear β -decay response corresponding to vanishing momentum transfer is only possible at much higher energies. For example, calculations for $^{12}\text{B}(1^+)$ at $E/A = 200 \text{ MeV}$ show that the tensor contribution is reduced to 5% at forward angles.

In summary, one-step direct and two-step transfer contributions to heavy-ion charge-exchange reactions have been studied theoretically as a function of incident energy. The calculations show that the reaction mechanism of heavy-ion charge-exchange scattering is changing from transfer to direct as the incident energy increases from $E/A = 10 \text{ MeV}$ to 100 MeV . However, the transition point depends on the final state. Generally, the two-step process can be neglected for $E/A \geq 100 \text{ MeV}$. Similar conclusions will hold for other (quasielastic) heavy-ion reactions at intermediate energies, thus indicating that mean-field processes vanish only at much higher incident energies as is usually expected.

Stimulating discussions with W. von Oertzen are gratefully acknowledged. This work was supported by Bundesministerium für Forschung und Technologie (Bonn, Germany) Grant No. 06ML177-8.

¹C. Gaarde, in *Nuclear Structure 1985: Proceedings of the Niels Bohr Centennial Conference, Copenhagen, Denmark, 20-25 May 1985*, edited by R. A. Broglia *et al.* (Elsevier, Amsterdam, 1985), p. 449.

²F. Selove-Ajzenberg, R. E. Brown, E. R. Flynn, and J. W. Sunier, *Phys. Rev. C* **31**, 777 (1985).

³F. Osterfeld, and H. H. Wolter, *Phys. Lett.* **60B**, 253 (1976).

⁴A. Etchegoyen, D. Sinclair, S. Liu, M. C. Etchegoyen, D. K. Scott, and D. L. Hendrie, *Nucl. Phys.* **A397**, 343 (1983).

⁵C. Brendel, P. von Neumann-Cosel, A. Richter, G. Schrieder, H. Lenske, H. H. Wolter, J. Carter, and D. Schüll, *Nucl. Phys.* **A477**, 162 (1988).

⁶H. G. Bohlen, B. Gebauer, A. Miczaika, W. von Oertzen, E. Stiliaris, H. Lenske, and H. H. Wolter, in *Proceedings of the Beijing International Symposium on Physics at Tandem, Beijing, 1986*, edited by C.-L. Jiang *et al.* (World Scientific, Singapore, 1987).

⁷J. S. Winfield, N. Anantaraman, S. M. Austin, L. H. Harwood, J. van der Plicht, H. L. Wu, and A. F. Zeller, *Phys. Rev. C* **33**, 1333 (1986).

⁸H. Lenske, *Nucl. Phys.* **A482**, 343c (1988); *Proceedings of the Fifth International Conference on Nuclear Reaction Mechanisms, Varenna, Italy, June 1988*, edited by E. Gadioli (Univ. Stud. di Milano, Milano, 1988).

⁹W. von Oertzen, *Nucl. Phys.* **A482**, 357c (1988).

¹⁰H. G. Bohlen *et al.*, *Nucl. Phys.* **A488**, 89c (1988).

¹¹G. R. Satchler, *Direct Nuclear Reactions* (Clarendon, Oxford, 1983).

¹²N. Anantaraman, H. Toki, and G. F. Bertsch, *Nucl. Phys.* **A398**, 269 (1982).

¹³W. G. Love and M. A. Franey, *Phys. Rev. C* **24**, 1073 (1981); M. A. Franey and W. G. Love, *Phys. Rev. C* **31**, 488 (1985).

¹⁴W. G. Love and G. R. Satchler, *Phys. Rep.* **55**, 183 (1979); W. G. Love, *Nucl. Phys.* **A312**, 160 (1978).

¹⁵T. Tamura, *Phys. Rep.* **14C**, 59 (1974); T. Tamura, T. Udagawa, and C. Mermaz, *Phys. Rep.* **65**, 345 (1980); T. Udagawa, H. H. Wolter, and W. R. Coker, *Phys. Rev. Lett.* **31**, 1507 (1973).

¹⁶M. Buenerd *et al.*, *Nucl. Phys.* **A424**, 313 (1984); H. G. Bohlen *et al.*, *Z. Phys. A* **322**, 241 (1985).

¹⁷W. von Oertzen, *Phys. Lett.* **151B**, 95 (1985).

¹⁸C. D. Goodman *et al.*, *Phys. Rev. Lett.* **44**, 1755 (1980); T. N. Taddeucci *et al.*, *Nucl. Phys.* **A469**, 125 (1987).